Amitriptyline at an environmentally relevant concentration alters the profile of metabolites beyond monoamines in gilt-head bream

Haizea Ziarrusta*†‡§, Anton Ribbenstedt§, Leire Mijangos†‡, Sergio Picart-Armada‖#††, Alex Perera-Lluna‖#††, Ailette Prieto†‡, Urtzi Izagirre‡, Jonathan P. Benskin§, Maitane Olivares†‡, Olatz Zuloaga†‡, Nestor Etxebarria†‡

†Department of Analytical Chemistry, University of the Basque Country (UPV/EHU), Leioa, Basque Country, Spain

‡Research Centre for Experimental Marine Biology and Biotechnology, University of the Basque Country (PiE-UPV/EHU), Plentzia, Basque Country, Spain

§Department of Environmental Science and Analytical Chemistry (ACES), Stockholm University, Stockholm, Sweden

‖B2SLab, Departament d'Enginyeria de Sistemes, Automàtica i Informàtica Industrial, Universitat Politècnica de Catalunya, Barcelona, Spain

#Networking Biomedical Research Centre in the subject area of Bioengineering, Biomaterials and Nanomedicine (CIBER-BBN), Madrid, Spain

††Institut de Recerca Pediàtrica Hospital Sant Joan de DeÂu, Esplugues de Llobregat, Barcelona, Spain

ABSTRACT

The antidepressant amitriptyline is a widely used selective serotonin reuptake inhibitor that is found in the aquatic environment. The present work investigates alterations in the brain and liver metabolome of gilt-head bream (*Sparus aurata*) following exposure at an environmentally relevant concentration (0.2 µg/L) of amitriptyline for 7 days. Analysis of variance-simultaneous component analysis (ASCA) was used to identify metabolites that distinguished exposed from control animals. Overall, alterations in lipid metabolism suggest the occurrence of oxidative stress in both brain and liver, a common adverse effect of xenobiotics. However, alterations in the amino acid arginine were also observed, likely related to the nitric oxide system, which is known to be associated with the mechanism of action of antidepressants. Additionally, changes on asparagine and methionine levels in brain and pantothenate, uric acid, formylisoglutamine/N-formimino-L-glutamate levels in liver could indicate alteration of amino acid metabolism in both tissues, and the perturbation of glutamate in liver suggests that the energy metabolism was also affected. These results revealed that environmentally relevant concentrations of amitriptyline perturbed a fraction of the metabolome which is not typically associated with antidepressant exposure in fish.

***Keywords*:** aquatic toxicology, fish, metabolomics, pharmaceuticals, antidepressant, multivariate statistics

**Address correspondence to* haizea.ziarrusta@ehu.eus

INTRODUCTION

Amitriptyline is the most prescribed tricyclic antidepressant for treatment of depression and several neuropathic and inflammatory illnesses (Calisto and Esteves 2009; Bautista-Ferrufino et al. 2011). Like other pharmaceuticals, amitriptyline and its by-products are incompletely removed during wastewater treatment (Lajeunesse et al. 2008), resulting in their occurrence in the natural environment. Amitriptyline concentrations of up to 72 ng/L have been reported in surface water (Kasprzyk-Hordern et al. 2008; Lajeunesse et al. 2008; Togola and Budzinski 2008), while concentrations up to 1.8 ng/g were observed in aquatic organisms (Klosterhaus et al. 2013; Ziarrusta et al. 2016).

In humans, therapeutic doses of amitriptyline (75 mg/day in adults), inhibit serotonin and norepinephrine reuptake in the presynaptic nerve endings, reducing hyperactivity of the hypothalamic-pituitary-adrenal (HPA) axis, which efficiently treats major depression (Moreno-Fernández et al. 2008). Vismari and co-workers (Vismari et al. 2012) also showed that amitriptyline inhibits the release of proinflammatory cytokines by immune cells, which decrease nitric oxide (NO) production. In mammals, adverse effects associated with amitriptyline have also been reported (Kitagawa et al. 2006; Lirk et al. 2006; Moreno-Fernández et al. 2008). For instance, amitriptyline-induced neurotoxicity was attributed to caspase-mediated apoptosis (Lirk et al. 2006) and to its chemical nature as a detergent (Kitagawa et al. 2006). Additionally, amitriptyline exposure also caused an increase of intracellular lipid peroxidation and the increase of reactive oxygen species (ROS), implying oxidative stress (Moreno-Fernández et al. 2008).

Occurrence of antidepressants in aquatic ecosystems and their potential effects on non-target organisms is of growing concern (Brooks et al. 2003; Johnson et al. 2007; Minagh et al. 2009; Guler and Ford 2010; Styrishave et al. 2011; Fong and Ford 2014). Although some authors have considered amitriptyline (Simmons et al. 2017; David et al. 2018), most studies investigating the hazards associated with antidepressants in aquatic organisms have focused on serotonin selective reuptake inhibitors (SSRIs) such as fluoxetine and venlafaxine (Clotfelter et al. 2007; Gaworecki and Klaine 2008; Winder et al. 2009; Bisesi Jr et al. 2014; Bisesi et al. 2016). These studies mainly focus on targeted endpoints related to the known mechanism of action of SSRIs, such as monoamine reuptake inhibition. However, SSRIs may also affect receptors unrelated to monoamine reuptake inhibition (e.g. 5-HT) (Stahl 1998), resulting in perturbation of other biochemical pathways such as energy metabolism, amino acid metabolism and hormone signalling (Webhofer et al. 2011). Studies involving tricyclic antidepressants in

aquatic organisms are largely non-existent, and to our knowledge, only a single aquatic toxicity study involving amitriptyline has been carried out (Yang et al. 2014). In that work, alterations to the HPA-axis and antioxidant system were observed at amitriptyline concentrations as low as 100 ng/L.

Investigating the effects of xenobiotics occurring in the environment at non-lethal levels is challenging since endpoints measured using standard toxicological assays are often incapable of detecting effects at such low levels. To this end, metabolomics - defined as the analysis of low molecular weight endogenous molecules in a biological sample (Viant 2008) - has proven useful by offering insight into early biochemical perturbations triggered at low dose, which may lead to an adverse effect (Huang et al. 2016). Metabolomics aims to identify specific biochemicals among the large number of metabolites in a sample that are capable of defining the case of study (Aoki-Kinoshita 2006; Wishart et al. 2007). Both univariate (Vinaixa et al. 2012; Shi et al. 2013) and multivariate (Shi et al. 2013; Worley and Powers 2013; Huang et al. 2016) approaches have been applied for metabolomics data treatment, where generally highly dimensional and multi-correlated data are obtained for a few replicate samples. However, both approaches have limitations. Univariate approaches such as analysis of variance (ANOVA) cannot account for covariance between variables. On the other hand, multivariate tools such as principal component analysis (PCA) are limited in terms of their ability to handle the underlying experimental design, and consequently, the variation caused by the experimental design can be confounded in the model (Jansen et al. 2005; Nueda et al. 2007). In order to overcome such limitations, ANOVA-simultaneous component analysis (ASCA) was introduced as a novel approach for the analysis of multivariate data from a designed experiment (e.g. the combination of dose and time). ASCA combines ANOVA with PCA to produce a data analysis method which accounts for both the covariance between multiple variables and the variation caused by the experimental design (Jansen et al. 2005). For example, multivariate ASCA method was applied by Malik et al. (Malik et al. 2016) to study alterations in the lipid profile of *Daphnia magna* exposed to tributyltin during its reproductive cycle, and by Gómez-Canela and co-workers (Gómez-Canela et al. 2017) to assess the toxic effects of chlorpyrifos in zebrafish.

The main objective of this work was to investigate time-dependent effects of amitriptyline in juvenile gilt-head bream (*Sparus aurata*) exposed to an environmentally relevant concentration. To achieve this goal, we measured overall perturbations in the

brain and liver metabolome using a multi-platform targeted/non-targeted metabolomic approach (Ribbenstedt et al. 2018) for a broad coverage of endogenous metabolites, allowing to identify the effects unrelated to monoamines. To our knowledge, this is the first study to investigate low-dose metabolic effects of amitriptyline in fish.

EXPERIMENTAL

Standards and Reagents

Amitriptyline hydrochloride (98%) was purchased from Sigma–Aldrich (St. Louis, MO, USA). A stock dosing solution of amitriptyline was prepared at 5000 mg/L in ethanol (EtOH) and diluted down to 85.2 µg/L in Milli-Q water for dosing purposes. The final concentration of EtOH in the tank was 0.0004‰. All stock solutions were stored at −20 °C prior to use. Additional information on reagents used is provided in the supplementary information (SI). Target abbreviations are provided in Table S1 of the SI and were adapted from Ribbenstedt et al. (Ribbenstedt et al. 2018). Glycerophospholipids were defined based on the presence of ester and/or ether bonds (represented by an 'a' or 'e', respectively), the length of fatty acid chain, and the number of double bonds. Two letters (ae = acyl-alkyl, aa = diacyl) were used to denote fatty acids bound to two glycerol positions, while carnitines were named according to the number of carbon atoms and double bonds. Lastly, sphingomyelins were denoted as SM with a C followed by the number of carbons in the fatty acid chain and the number of double bonds.

Amitriptyline exposure experiments

Juvenile gilt-head bream weighing ~40 g and measuring ~13 cm in length were obtained from Groupe Aqualande (Roquefort, France) and shipped to the Research Centre for Experimental Marine Biology and Biotechnology (PiE-UPV/EHU), where exposure experiments were carried out. The exposure laboratory was maintained at 18 °C and a 14:10 h light:dark cycle, and water temperature (13.5 ± 0.5 ˚C) and pH (7.3 ± 0.3) were constant throughout the entire experiment. Fish were acclimatized for two weeks upon arrival, and then stabilized for an additional 48 hours in the dosing tanks before the exposure. The water was continuously aerated and fish were fed daily with 0.10 g pellets/fish (EFICO YM 868, 3 mm, BioMar Group, Denmark). Dissolved oxygen, nitrite, nitrate and ammonium were measured periodically during the exposure period to confirm water quality.

The present work was conducted in parallel with a bioaccumulation/biotransformation study, and sampling and dissection details are explained elsewhere (Ziarrusta et al. 2017). Fish processing described herein was evaluated by the Bioethics Committee of UPV/EHU and approved by the Local Authority according to the current regulations (procedure approval CEEA/380/2014/ETXEBARRIA LOIZATE). A 7-day environmentally relevant exposure (0.2 µg/L nominal) was performed using two 1000 × 700 × 650 mm polypropylene tanks (one control, one exposed), each containing 250 L of seawater and 145 fish. Exposures were carried out using a continuous flow-through system with a peristaltic pump delivering 8.5 L seawater/h and another pump infusing an amitriptyline stock solution at 20 mL/h to exposure tanks. Amitriptyline stock dosing solutions were refilled every 48 hours. Control tanks were maintained at identical conditions as exposed tanks, and 10 fish were collected from each tank before starting the dosing (day 0) and on exposure days 2, 4 and 7. Taking into account the number of fish and tanks available for the experiment, it was possible to have within-tank replicates (i.e. biological replicates per condition), but between-tank replicates (i.e. condition replicates) could not be run. Lastly, we collected and analyzed water the same sampling days fish were collected and the time-weighted average concentration was calculated (0.12 ± 0.02 µg/L) as the mean concentration of the four sampling days.

Extraction and analysis of metabolites

Sample treatment and instrumental analysis. Metabolite extraction and analysis were carried out using a previously optimized and validated analytical method (Ribbenstedt et al. 2018). Extraction of the whole tissues was initiated through addition of 5 µL $CHCl_3$:MeOH (20:80, v/v) per mg tissue in 1.5 mL tubes for brain and 13 mL polypropylene tubes for liver, employing ZrO beads (2.0 mm for brain and 4.8 mm for liver) purchased from Next Advance (New York, United States). All samples were homogenized for 4 min at 1500 rpm, using a 1600 MiniG homogenizer (Spex Sample Prep, New Jersey, USA). Two dilutions for each brain sample (1:5 and 1:100) and liver sample (1:15 and 1:300) were carried out with pure MeOH and an internal standard solution was added (200 µg/L in the diluted extract), prior to instrumental analysis (Ribbenstedt et al. 2018).

Metabolomic analysis was carried out at ACES-Stockholm University, combining targeted and non-targeted approaches described elsewhere (Ribbenstedt et al. 2018). Briefly, targeted analysis of diluted extracts of both brain and liver was carried out performing 2 runs per extract (aliquots of 5 µL): (i) by ultra high performance liquid

chromatography coupled to triple quadrupole mass spectrometry (UHPLC-QqQ-MS/MS) acquiring the mass spectra simultaneously in positive and negative mode and using a hydrophilic interaction liquid chromatography (HILIC) column, and (ii) by flow injection-QqQ-MS/MS. With these analyses we monitored a total of 181 metabolites, including 18 amino acids, 11 biogenic amines, 5 neurotransmitters, 5 nucleobases, 50 carnitines, 67 phosphatidylcholines, 16 lysophosphatidylcholines and 9 sphingomyelins (Ribbenstedt et al. 2018). Although the better analytical precision and unequivocal identification of targeted analysis enhances the potential to detect statistically significant perturbations in the metabolome, the metabolic coverage can be increased by means of non-targeted analysis. Therefore, the less diluted extracts of each matrix (1:5 and 1:15 for brain and liver extracts, respectively) were analyzed by means of UHPLC coupled to tandem quadrupole-Orbitrap (UHPLC-qOrbitrap) high resolution mass spectrometry (HRMS) (Ribbenstedt et al. 2018). In order to maximize metabolite coverage in this untargeted approach, 4 runs were performed per extract (aliquots of 5 µL) using two different chromatographic columns (one HILIC column and one reverse-phase octadecylsilyl (C18)) and two ionization modes, positive ($HILIC_{pos}$ and $C18_{pos}$) and negative ($HILIC_{neg}$ and $C18_{neg}$).

Quality control samples. In this work, instrumental blank samples (pure MeOH) were injected every 5 samples to monitor carryover, and a set of procedural blanks were prepared to estimate the background concentration of metabolites during sample workup. In addition, two sets of quality control samples were prepared. First, an extraction quality control sample (QC_{ext}) was prepared by pooling aliquots of individual tissues (n=20). Portions of this pool were included in different extraction batches in order to check for extraction reproducibility. Second, a sequence quality control sample (QC_{seq}) was prepared for each tissue by pooling a small volume of each extract and splitting into several aliquots. These aliquots were injected after every 10 samples to monitor and correct for signal drift.

The extraction and analysis of samples was randomized and the samples were analyzed in six runs/sequences (including samples, QCs, pure MeOH and standard solutions) per tissue: two for targeted analysis (UHPLC-QqQ-MS/MS and flow injection- QqQ -MS/MS) and another four for non-targeted ($HILIC_{pos}$, $HILIC_{neg}$, $C18_{pos}$ and $C18_{neg}$ in UHPLC-qOrbitrap). No carryover was observed along the sequences.

Data Handling and Statistical Analyses

As a general assessment of fish health, condition factor (K) (Fulton 1904) and hepatic-somatic index (HSI) were determined using Equations 1 and 2, respectively.

$$K = \frac{Fish\,weight\ x\,100}{Fish\,length^3}$$

Equation 1

$$HSI = \frac{Liver\ weight\ x\,100}{Fish\ weight}$$

Equation 2

K and HSI were statistically evaluated between exposed and control groups using two-way ANOVA. Identification of putative metabolites involved in altered metabolic pathways was performed separately for brain and liver tissues in both targeted and non-targeted approaches.

Statistical data treatment in targeted analysis. Metabolites of interest were detected and quantified using the XCalibur 4.0 software. Prior to statistical analysis the data set was filtered and those metabolites displaying concentrations under the limit of detection (i.e. missing values) in more than 50% of the samples were removed. This filtering was evenly distributed between the exposed and control groups. For the remaining metabolites, the *K*-nearest neighbour (KNN) imputation method was used to estimate the remaining missing values (Hrydziuszko and Viant 2012).

Although QC_{ext} data were consistent across all batches, signal drift (identified from QC_{seq} data) was observed (see Figure S1 for proline meabolite as an example), and it could not be corrected using internal standards. Consequently, a Feature-Based Signal Correction (FBSC) was applied using Equation 3 (Kamleh et al. 2012), where $x'_{i,j}$ is the corrected peak area of the feature i in the sample j and $x_{i,j}$ is the peak area without modifications. The correction factor $f_{i,j}$ was calculated as the theoretical value of the peak area interpolating the order of injection in the regression curve of this feature in the QC_{seq} samples. The result was multiplied by $x'_{i,1}$ which is the corrected signal for feature i in the first QC_{seq} sample (j=1) in order to recover the original dimensions of the features (Kamleh et al. 2012).

$$x'_{i,j} = \frac{x_{i,j}}{f_{i,j}} \cdot x'_{i,1}$$

Equation 3

In order to identify metabolites involved in altered metabolic pathways, the corrected data acquired in both sequences (i.e., UHPLC-MS/MS and flow injection-MS/MS) were

merged and treated in the same statistical analysis workflow. The data were autoscaled to provide equal variance to each variable and outliers were identified based on Principal Components Analysis (PCA).(Simmons et al. 2015; Gorrochategui et al. 2016) The samples that were out of the 95% confidence regions of the whole dataset were discarded.

The whole dataset was analyzed by multiple linear regression analysis (MLR, Y (time, dose) = time + dose + time·dose, where Y is feature response) using R software for statistical computing (v3.4.3). The *p-values* were computed through the default "summary.lm" function in the stats R package. Since the objective was to identify metabolites displaying statistically significant concentration changes over time between exposed and control samples, we paid special attention to the interaction between dose and time (i.e. dose·time). After applying linear analysis and multiple testing we selected metabolites with a *p-value* < 0.05 and a *false discovery rate (FDR)* < 0.05 in the interaction dose·time.

Additionally, since the current study employed a 2-factor experimental design (exposure time, days 0, 2, 4 and 7, and dosing concentration, control and exposed), the ASCA approach was applied, using MetaboAnalyst 3.5 (Xia et al. 2015). ASCA splits the overall data variance into individual variances induced by each factor and their interaction. The algorithm uses two parameters to predict the behaviour of features within the submodels built for the two factors and their interaction, the leverage, and the squared prediction error (SPE) (Nueda et al. 2007). While the leverage measures the importance of a feature in the ASCA model, SPE is a measure of the goodness of the model fit for each specific metabolite. Hence, meaningful metabolites will be those showing a high leverage (leverage threshold > 0.85) and low SPE (alpha threshold < 0.05). For those meaningful metabolites, we calculated daily fold-change (FC) values according to Equation 4, by dividing the average concentration of the metabolite *j* in the exposed samples at day *i* with the average concentration of the metabolite *j* in the control samples at day *i*:

$$Fold-change\,(FC)_{day\,i,\,metabolite\,j} = \frac{j\,concentration_{exposed\,sample\,at\,day\,i}}{j\,concentration_{control\,sample\,at\,day\,i}} \qquad \text{Equation 4}$$

Statistical data treatment in non-targeted analysis. Chromatograms acquired in non-targeted analysis were processed using Compound Discoverer 2.1 (Thermo-Fisher Scientific). The full workflow and settings for non-targeted analysis are found in SI.

Thereafter, each data set was filtered to keep only endogenous metabolites by searching the detected exact masses in a database containing up to 4400 endogenous compounds or in LipidMaps (http://www.lipidmaps.org/).

Similar to targeted analysis, outliers were discarded by means of PCA, and signal drift over the course of the sequence had to be corrected. Since the FBSC approach did not correct for signal drift completely in the non-targeted analysis, signal drift over the course of each sequence was corrected using the intCor package (Fernández-Albert et al. 2014) in the R software for statistical computing (v3.4.3). To create the model we defined the three classes (i.e., control, exposed and QC_{seq}) and the number of components of the model in each specific sequence. Signal correction was performed via a two-step approach that combines Common Principal Components Analysis (CPCA) and the medians method. Similar to targeted analysis, QC_{ext} data were consistent across all batches after signal drift correction. Moreover, after signal drift correction along each sequence, the data collected in the four sequences ($HILIC_{pos}$, $HILIC_{neg}$, $C18_{pos}$, $C18_{neg}$) in non-targeted analysis was merged in one file and analysed altogether, in order to study dose·time interaction through MLR and to select the features that passed the criteria of *p-value* < 0.05 and *FDR* < 0.05 in the multiple testing method (see *Statistical data treatment in targeted analysis*). Additionally, ASCA was also used for the statistical analysis of non-targeted data and those features with a *leverage threshold* higher than 0.85 and *SPE* lower than 0.05 were selected as meaningful features.

In the case of non-targeted data treatments, significant features were manually checked to discard those peaks with bad chromatographic peak shape and/or those which were incorrectly integrated, as well as the peaks that corresponded to amitriptyline by-products so as to avoid statistical and/or biological misinterpretation of the data (Ziarrusta et al. 2017). Then, FC values were calculated according to Equation 4, and metabolite identification (Fiehn et al. 2007; Schymanski et al. 2014) was carried out using the following approach. When available, the exact mass, isotopic profile, fragmentation and abundances were compared with those in the mzCloud library (Thermo) for metabolite annotation. In cases where the metabolite was not included in the mzCloud library, tentative candidates were searched for in other databases such as KEGG (http://www.kegg.jp/kegg/) and LipidMaps (http://www.lipidmaps.org/) and, then, experimental fragmentation patterns were compared against the *in silico*

fragmentation obtained in MetFrag (https://msbi.ipb-halle.de/MetFragBeta/) in order to select the most plausible metabolite.

RESULTS AND DISCUSSION

General health condition parameters

No significant changes in fish weight and length were observed at the 95% confidence level, regardless of amitriptyline dose or exposure time (*p-value* = 0.25 and 0.66, for fish weight and length, respectively). There was no mortality and K and HSI were comparable between fish of exposed and control groups (*p-value* = 0.50 and 0.42, respectively) throughout the experiment.

Perturbation in the metabolome

In both targeted and non-targeted results, by means of MLR, no metabolite passed the *FDR* < 0.05 cut-off. Although amitriptyline was accumulated in gilt-head bream (Ziarrusta et al. 2017), the much lower amitriptyline exposure concentration used in this work (0.2 ng/mL) compared to other studies in the literature on antidepressants (23-465 µg/L) (Gaworecki and Klaine 2008; Bisesi Jr et al. 2014; Bisesi et al. 2016) might have caused the metabolic alterations not to be significant enough to be detected by MLR analysis. However, by means of ASCA, we evaluated separately the statistical significances of the two categorical factors (dose and exposure time) and of their interaction, and significant metabolic perturbations were observed in both targeted and non-targeted results.

Targeted results. Both time and dose·time interaction submodels passed the permutation test (*p-value* < 0.05) in brain and liver (see Table 1), while the dose submodels (*p-value* > 0.05) did not pass the permutation test using 1000 permutations. The first 2 PCs explain almost the 90% of the variance for both time and dose·time interaction submodels. According to ASCA, exposure time was the most significant variable to perturb metabolites levels in both liver and brain (lowest *p-values* for time submodels). The time dependent alteration of some metabolite profiles (i.e., lysine, glutamine, phenylalanine in both matrices, as well as adenine, tyrosine, proline, malic acid, C3, C18:2, C12:1-OH, C14, C16:2-OH, C16:1-OH, C12, C14:2, and PCaeC38 in brain, and alloisoleucine, valine, arginine, PCaaC40:6 and PCaeC38:1 in liver) in both exposed and control animals could be related to experimental conditions such as the reduction in the number of fish in both tanks as the experiment progressed.

Additionally, from the dose·time interaction submodels we identified the most significant dose-related effects. As it can be observed in Figure 1A and Figure 1B, which show the scores diagrams of the first PC1 in submodel dose·time, the greatest differences between dose groups were observed on the last day of exposure (day 7) for both matrices. For these significantly altered target metabolites after exposure according to ASCA, daily FC values are shown in Figure 2. Additionally, in the same figure, the significance level between exposed and control samples calculated through a t-test is included.

In the case of liver, the results of the dose·time submodel showed that the concentrations in control and exposed animals were altered differently during the experiment for 13 metabolites, including, methionine, glutamate and other 11 lipidic metabolites such as acylcarnitines (C18, C17:1-COOH, C16:1-OH and C5), phosphatidylcholines (PCaaC30:2, PCaaC32:1, PCaaC32:2 and PCaaC32:3), lysoPCs (lysoPCa20:3 and lysoPCa24:1) and one sphingomyelin (SM C18:1). On the other hand, in brain tissue 10 metabolites were altered according to dose·time interaction submodel, including, arginine, methionine, asparagine and other 7 lipidic metabolites such as C4 acyl carnitine, 3 PCs (PCaeC34:1, PCae C36:3 and PCae C38:2), 2 lysoPCs (lysoPCa C16:0 and lysoPCa C18:1) and the SM C18:0.

Non-targeted results. As was the case with the targeted data, ASCA dose submodels built using the features identified in brain and liver extracts, did not pass permutation testing (*p-value* >0.05) whereas the lowest *p-values* were achieved for time submodels (see Table 1). These results indicate that the exposure time was the most significant variable in the exposure experiments performed with amitriptyline. Regarding the dose·time submodels, the permutation test only passed for liver (see Table 1). Additionally, as it can be observed in Figure 1C, the most profound alterations were observed on the last day of exposure (day 7), consistent with the targeted results. The results of the dose·time submodel showed that the concentrations of control and exposed animals were altered differently during the experiment for 37 features (see Table 2). From those 37 features/metabolites, only 3 were KEGG annotated, since the other 34 were putatively identified as lipids not included in KEGG. Notably, the few KEGG annotated metabolites ruled out the possibility of performing pathway enrichment (Chagoyen and Pazos 2013). Furthermore, even though in most cases it was not possible to specify the exact structure of the lipid due to the existence of different isomers, we

were able to indicate the lipid category to which they belong to (see Table 2). Among the 34 tentatively identified lipids there are 1 fatty acyl, 3 sphingolipids, 2 sterol lipids, 25 glycerophospholipids and 3 glycerolipids. Fold change values for all 37 significantly altered features at exposure days 2, 4 and 7 are also provided in Table 2, together with the significance level between exposed and control samples calculated through a t-test is included.

In the case of liver, significant dose·time submodels were observed in both targeted and non-targeted results, the main similarity between targeted and non-targeted approaches was that most of the significantly altered concentrations are of lipidic metabolites (11 out of 13 and 34 out of 37 in targeted and non-targeted analysis, respectively). However, only the acyl carnitine C18, also known as stearoylcarnitine, was identified by both approaches (Figure 3). This could be due to greater variability (i.e. higher standard deviation) in non-target analysis compared to targeted analysis (Ribbenstedt et al. 2018).

Biological interpretation of dose-related effects

Metabolites identified by ASCA to be significantly altered by amitriptyline exposure were used for the biological interpretation (targeted or non-targeted data). Overall, the most significant dose-related effects regardless of tissue were observed for arginine, methionine, glutamate, asparagine, pantothenate, uric acid, formylisoglutamine/N-formimino-L-glutamate and 51 metabolites belonging to lipid metabolism.

The alteration in arginine levels in brain may be related to a perturbation in enzymatic production of nitric oxide (NO) since it has been reported that antidepressant treatments regulate the NO system (Park et al. 2017). In fact, NO synthase catalyses transformation of arginine to citrulline resulting in NO production as a by-product. According to the literature, SSRIs might bind to NO synthase (Stahl 1998; Yaron et al. 1999). Furthermore, other studies have reported a reduction of NO content in zebrafish embryos exposed to amitriptyline at concentrations below 1 mg/L (Yang et al. 2014). Therefore, the alteration in arginine observed in the present work may be a sign of oxidative stress-protecting activity, which is consistent with a study with rats that revealed that the antidepressant effect of fluoxetine is associated with a decreased production of ROS (Rebai et al. 2017).

As observed in Figure 2B, accumulation of longer chain acyl carnitines in the liver of exposed fish (FC > 1.50) may be a sign of hepatic oxidative stress, a common adverse effect of xenobiotics (Kotarsky et al. 2012; Gómez-Canela et al. 2017). The metabolism

of amitriptyline by hepatic CYP-enzymes (Breyer-Pfaff 2004) is a plausible explanation for this increase in ROS and, consistent with this hypothesis, amitriptyline was mainly metabolized to monohydroxylated compounds in exposed fish liver (Ziarrusta et al. 2017). Additionally, similar to Kotarsky and co-workers' observations (Kotarsky et al. 2012), this effect was not observed for carnitine or for shorter chain acylcarnitines in the present work, and only the levels of longer chain acylcarnitines increased in the exposed fish liver. Overall, a significant positive correlation was observed between acyl carnitine chain length and exposed/control ratio (r^2=0.76; Figure 4), which may suggest an over-consumption of reserve lipids (Gómez-Canela et al. 2017).

The results included in Figure 2 and Table 2 suggest that amino acid metabolism in both tissues was altered in the presence of amitriptyline since methionine and asparagine and pantothenate, uric acid, formylisoglutamine/N-formimino-L-glutamate were altered in brain and liver tissues, respectively. The alteration of methionine, which is a carnitine precursor, and asparagine levels is consistent with the observations in rats exposed to the tricyclic antidepressant imipramine described elsewhere (Nagasawa et al. 2015), in which significant perturbations in brain concentrations of methionine, asparagine, glutamate, and other amino acids were observed. Alterations in amino acid metabolism in the brain have been related to stress vulnerability in rats (Murakami et al. 2009; Nagasawa et al. 2012). Additionally, we also observed perturbation of the amino acid metabolism in liver with concentration alterations of metabolites that belong to β-alanine metabolism, purine metabolism and histidine metabolism.

Glutamate plays an important role in amino acid metabolism in liver. It is a precursor to glutathione and is produced during catabolism of folate coenzymes and during the removal of GABA (Brosnan and Brosnan 2009). The alteration that we observed in the concentration of glutamate in fish liver might be associated to energy metabolism since glutamate is transformed by glutamate dehydrogenase into α-ketoglutarate, which is a Krebs cycle intermediate. This result reveals that amitriptyline may alter amino acids related with the energy metabolism, similar to the effects observed for the SSRI paroxetine (Webhofer et al. 2011), and beyond the most widely investigated monoamines in SSRI drug studies (Gaworecki and Klaine 2008; Winder et al. 2009; Bisesi Jr et al. 2014; Bisesi et al. 2016).

The lower levels in liver lysoPCs in exposed animals relative to controls (FC < 1.00 the last day of exposure) suggested that amitriptyline might result in increased turnover of lysoPCs in exposed animals. Indeed, Xia and co-workers reported that cationic

amphiphilic drugs such as amitriptyline induce phospholipidosis (i.e., lipid storage disorders) in cells of most organs (Xia et al. 2000). Moreover, lysoPCs are known to be blood biomarkers for drug-induced hepatic phospholipidosis (Saito et al. 2014). In addition to the lysoPCs (lysoPCa20:3 and lysoPCa24:1) and PCs (PCaaC30:2, PCaaC32:1, PCaaC32:2 and PCaaC32:3) identified from targeted analysis, as it can be observed in Table 2, another 25 glycerophospholipids, 3 glycerolipids, 2 sterol lipids and 3 sphingolipids were also identified as significantly altered in the non-targeted analysis. Overall, these alterations observed in the present work are in accordance with recent metabolomic study that reported an association between changes in lipids and oxidative stress (Zhao et al. 2015).

Lipid metabolism was also perturbed in brain, yet in contrast to liver, all lipid classes (i.e. acylcarnitines, lysoPCs, PCs and SMs) displayed a significant concentration increase on the 7th day of exposure (FC > 1.00 in all the cases). SSRIs are known to bind to phospholipids and such binding may alter the lipid's suitability as a substrate for phospholipases (Xia et al. 2000), which may explain the observed increase in PCs. On the other hand, tricyclic antidepressants, including amitriptyline, inhibit sphingomyelinase activity (Albouz et al. 1986), causing accumulation of sphingomyelins. An inverse correlation between phosphatidylcholines and sphingolipids and neurological disorders (anxiety and depression) has also been observed in the literature (Demirkan et al. 2013).

CONCLUSIONS

The present study showed that despite an absence of mortality or alterations in general health condition, environmentally relevant concentrations of amitriptyline can produce significant metabolic perturbations in both brain and liver of fish in only 7 days of exposure. The observed accumulation of longer chain acyl carnitines and alterations in compounds associated with lipid metabolism point to lipid storage disorders previously reported as an adverse effect of SSRIs which may be associated with oxidative stress commonly caused by xenobiotics (Gómez-Canela et al. 2017). However, SSRIs are also known to induce oxidative stress-protective activities through separate mechanisms, and in fact, the observed alteration in arginine could be associated with the decrease in enzymatic production of NO. Additionally, a carnitine-precursor, methionine, was perturbed in both liver and brain. However, the alterations of methionine and other amino acids were indicative of amino acid metabolism alteration, in good agreement

with the literature (Nagasawa et al. 2015). The variation of glutamate levels in liver suggests alteration in energy metabolism, as previously observed in other antidepressant studies (Webhofer et al. 2011). Collectively, these observations are notable since prior effects at the biochemical level (e.g. oxidative stress and energy metabolism alteration) have been connected to adverse effects at both the individual (growth impairment) and population levels (reduced survival) in fish (Groh et al. 2015).

Overall, these data indicate that amitriptyline exposure at environmentally relevant concentrations results in significant changes to the metabolome of fish. Furthermore, changes were observed in metabolites other than simply monoamines, which are the most commonly reported endpoint associated with amitriptyline exposure. Although these observations increase the limited available knowledge on the effects of AMI in non-target species such as fish, future work will include higher-dose and longer term exposure assays.

SUPPLEMENTAL DATA

This article includes online Supplemental Data.

ACKNOWLEDGEMENTS

This work was financially supported by the Ministry of Economy and Competitiveness through the project CTM2014-56628-C3-1-R and by the Basque Government through the project IT-742-13, and by ACES-Stockholm University (JPB). H. Ziarrusta and L. Mijangos are grateful to the Spanish Ministry and Basque Government for their pre-doctoral fellowships.

The authors declare no conflict of interest.

DATA AVAILABILITY

Please contact the corresponding author (haizea.ziarrusta@ehu.eus) for access to data.

REFERENCES

Albouz S, Le Saux F, Wenger D, Hauw JJ, Baumann N. 1986. Modifications of sphingomyelin and phosphatidylcholine metabolism by tricyclic antidepressants and phenothiazines. Life Sci. 38(4):357–363.

Aoki-Kinoshita KF. 2006. Overview of KEGG applications to omics-related research. J Pestic Sci. 31(3):296–299. doi:10.1584/jpestics.31.296.

Bautista-Ferrufino MR, Cordero MD, Sánchez-Alcázar JA, Illanes M, Fernández-Rodríguez A, Navas P, de Miguel M. 2011. Amitriptyline induces coenzyme Q deficiency and oxidative damage in mouse lung and liver. Toxicol Lett. 204(1):32–37. doi:10.1016/j.toxlet.2011.03.033.

Bisesi JH, Sweet LE, van den Hurk P, Klaine SJ. 2016. Effects of an antidepressant mixture on the brain serotonin and predation behavior of hybrid striped bass. Environ Toxicol Chem. 35(4):938–945. doi:10.1002/etc.3114.

Bisesi Jr JH, Bridges W, Klaine SJ. 2014. Effects of the antidepressant venlafaxine on fish brain serotonin and predation behavior. Aquat Toxicol. 148:130–138. doi:10.1016/j.aquatox.2013.12.033.

Breyer-Pfaff U. 2004. The Metabolic Fate of Amitriptyline, Nortriptyline and Amitriptylinoxide in Man. Drug Metab Rev. 36(3–4):723–746. doi:10.1081/DMR-200033482.

Brooks BW, Foran CM, Richards SM, Weston J, Turner PK, Stanley JK, Solomon KR, Slattery M, La Point TW. 2003. Aquatic ecotoxicology of fluoxetine. Toxicol Lett. 142(3):169–183. doi:10.1016/S0378-4274(03)00066-3.

Brosnan ME, Brosnan JT. 2009. Hepatic glutamate metabolism: a tale of 2 hepatocytes. Am J Clin Nutr. 90(3):857S-861S. doi:10.3945/ajcn.2009.27462Z.

Calisto V, Esteves VI. 2009. Psychiatric pharmaceuticals in the environment. Chemosphere. 77(10):1257–1274. doi:10.1016/j.chemosphere.2009.09.021.

Chagoyen M, Pazos F. 2013. Tools for the functional interpretation of metabolomic experiments. Brief Bioinform. 14(6):737–744. doi:10.1093/bib/bbs055.

Clotfelter ED, O'Hare EP, McNitt MM, Carpenter RE, Summers CH. 2007. Serotonin decreases aggression via 5-HT1A receptors in the fighting fish Betta splendens. Pharmacol Biochem Behav. 87(2):222–231. doi:10.1016/j.pbb.2007.04.018.

David A, Lange A, Tyler CR, Hill EM. 2018. Concentrating mixtures of neuroactive pharmaceuticals and altered neurotransmitter levels in the brain of fish exposed to a

524wastewater effluent. Sci Total Environ. 621:782–790.
525doi:10.1016/j.scitotenv.2017.11.265.

526Demirkan A, Isaacs A, Ugocsai P, Liebisch G, Struchalin M, Rudan I, Wilson JF,
527Pramstaller PP, Gyllensten U, Campbell H, et al. 2013. Plasma phosphatidylcholine and
528sphingomyelin concentrations are associated with depression and anxiety symptoms in a
529Dutch family-based lipidomics study. J Psychiatr Res. 47(3):357–362.
530doi:10.1016/j.jpsychires.2012.11.001.

531Fernández-Albert F, Llorach R, Garcia-Aloy M, Ziyatdinov A, Andres-Lacueva C,
532Perera A. 2014. Intensity drift removal in LC/MS metabolomics by common variance
533compensation. Bioinformatics. 30(20):2899–2905. doi:10.1093/bioinformatics/btu423.

534Fiehn O, Robertson D, Griffin J, van der Werf M, Nikolau B, Morrison N, Sumner LW,
535Goodacre R, Hardy NW, Taylor C, et al. 2007. The metabolomics standards initiative
536(MSI). Metabolomics. 3(3):175–178. doi:10.1007/s11306-007-0070-6.

537Fong PP, Ford AT. 2014. The biological effects of antidepressants on the molluscs and
538crustaceans: A review. Aquat Toxicol. 151:4–13. doi:10.1016/j.aquatox.2013.12.003.

539Fulton WT. 1904. The rate of growth of fishes. 22nd Annu Rep Fish Board Scotl.
5403:141–241.

541Gaworecki KM, Klaine SJ. 2008. Behavioral and biochemical responses of hybrid
542striped bass during and after fluoxetine exposure. Aquat Toxicol. 88(4):207–213.
543doi:10.1016/j.aquatox.2008.04.011.

544Gómez-Canela C, Prats E, Piña B, Tauler R. 2017. Assessment of chlorpyrifos toxic
545effects in zebrafish (Danio rerio) metabolism. Environ Pollut. 220, Part B:1231–1243.
546doi:10.1016/j.envpol.2016.11.010.

547Gorrochategui E, Jaumot J, Lacorte S, Tauler R. 2016. Data analysis strategies for
548targeted and untargeted LC-MS metabolomic studies: Overview and workflow. TrAC
549Trends Anal Chem. 82:425–442. doi:10.1016/j.trac.2016.07.004.

550Groh KJ, Carvalho RN, Chipman JK, Denslow ND, Halder M, Murphy CA, Roelofs D,
551Rolaki A, Schirmer K, Watanabe KH. 2015. Development and application of the
552adverse outcome pathway framework for understanding and predicting chronic toxicity:

553II. A focus on growth impairment in fish. Chemosphere. 120:778–792.
554doi:10.1016/j.chemosphere.2014.10.006.

555Guler Y, Ford AT. 2010. Anti-depressants make amphipods see the light. Aquat Toxicol.
55699(3):397–404. doi:10.1016/j.aquatox.2010.05.019.

557Hrydziuszko O, Viant MR. 2012. Missing values in mass spectrometry based
558metabolomics: an undervalued step in the data processing pipeline. Metabolomics.
5598(1):161–174. doi:10.1007/s11306-011-0366-4.

560Huang SSY, Benskin JP, Chandramouli B, Butler H, Helbing CC, Cosgrove JR. 2016.
561Xenobiotics Produce Distinct Metabolomic Responses in Zebrafish Larvae (Danio
562rerio). Environ Sci Technol. 50(12):6526–6535. doi:10.1021/acs.est.6b01128.

563Jansen JJ, Hoefsloot HCJ, van der Greef J, Timmerman ME, Westerhuis JA, Smilde AK.
5642005. ASCA: analysis of multivariate data obtained from an experimental design. J
565Chemom. 19(9):469–481. doi:10.1002/cem.952.

566Johnson DJ, Sanderson H, Brain RA, Wilson CJ, Solomon KR. 2007. Toxicity and
567hazard of selective serotonin reuptake inhibitor antidepressants fluoxetine, fluvoxamine,
568and sertraline to algae. Ecotoxicol Environ Saf. 67(1):128–139.
569doi:10.1016/j.ecoenv.2006.03.016.

570Kamleh MA, Ebbels TMD, Spagou K, Masson P, Want EJ. 2012. Optimizing the Use of
571Quality Control Samples for Signal Drift Correction in Large-Scale Urine Metabolic
572Profiling Studies. Anal Chem. 84(6):2670–2677. doi:10.1021/ac202733q.

573Kasprzyk-Hordern B, Dinsdale RM, Guwy AJ. 2008. The occurrence of
574pharmaceuticals, personal care products, endocrine disruptors and illicit drugs in surface
575water in South Wales, UK. Water Res. 42(13):3498–3518.
576doi:10.1016/j.watres.2008.04.026.

577Kitagawa N, Oda M, Nobutaka I, Satoh H, Totoki T, Morimoto M. 2006. A proposed
578mechanism for amitriptyline neurotoxicity based on its detergent nature. Toxicol Appl
579Pharmacol. 217(1):100–106. doi:10.1016/j.taap.2006.08.003.

580Klosterhaus SL, Grace R, Hamilton MC, Yee D. 2013. Method validation and
581reconnaissance of pharmaceuticals, personal care products, and alkylphenols in surface

582waters, sediments, and mussels in an urban estuary. Environ Int. 54:92–99.
583doi:10.1016/j.envint.2013.01.009.

584Kotarsky H, Keller M, Davoudi M, Levéen P, Karikoski R, Enot DP, Fellman V. 2012.
585Metabolite Profiles Reveal Energy Failure and Impaired Beta-Oxidation in Liver of
586Mice with Complex III Deficiency Due to a BCS1L Mutation. PLoS ONE. 7(7).
587doi:10.1371/journal.pone.0041156.

588Lajeunesse A, Gagnon C, Sauvé S. 2008. Determination of Basic Antidepressants and
589Their N-Desmethyl Metabolites in Raw Sewage and Wastewater Using Solid-Phase
590Extraction and Liquid Chromatography−Tandem Mass Spectrometry. Anal Chem.
59180(14):5325–5333. doi:10.1021/ac800162q.

592Lirk P, Haller I, Hausott B, Ingorokva S, Deibl M, Gerner P, Klimaschewski L. 2006.
593The neurotoxic effects of amitriptyline are mediated by apoptosis and are effectively
594blocked by inhibition of caspase activity. Anesth Analg. 102(6):1728–1733.
595doi:10.1213/01.ane.0000216018.62549.bb.

596Malik A, Jordao R, Campos B, Casas J, Barata C, Tauler R. 2016. Exploring the
597disruptive effects of TBT on lipid homeostasis of Daphnia magna using chemometric
598methods. Chemom Intell Lab Syst. 159(Supplement C):58–68.
599doi:10.1016/j.chemolab.2016.08.010.

600Minagh E, Hernan R, O'Rourke K, Lyng FM, Davoren M. 2009. Aquatic ecotoxicity of
601the selective serotonin reuptake inhibitor sertraline hydrochloride in a battery of
602freshwater test species. Ecotoxicol Environ Saf. 72(2):434–440.
603doi:10.1016/j.ecoenv.2008.05.002.

604Moreno-Fernández AM, Cordero MD, de Miguel M, Delgado-Rufino MD, Sánchez-
605Alcázar JA, Navas P. 2008. Cytotoxic effects of amitriptyline in human fibroblasts.
606Toxicology. 243(1):51–58. doi:10.1016/j.tox.2007.09.021.

607Murakami T, Yamane H, Tomonaga S, Furuse M. 2009. Forced swimming and
608imipramine modify plasma and brain amino acid concentrations in mice. Eur J
609Pharmacol. 602(1):73–77. doi:10.1016/j.ejphar.2008.10.049.

Nagasawa M, Ogino Y, Kurata K, Otsuka T, Yoshida J, Tomonaga S, Furuse M. 2012. Hypothesis with abnormal amino acid metabolism in depression and stress vulnerability in Wistar Kyoto rats. Amino Acids. 43(5):2101–2111. doi:10.1007/s00726-012-1294-y.

Nagasawa M, Otsuka T, Yasuo S, Furuse M. 2015. Chronic imipramine treatment differentially alters the brain and plasma amino acid metabolism in Wistar and Wistar Kyoto rats. Eur J Pharmacol. 762:127–135. doi:10.1016/j.ejphar.2015.05.043.

Nueda MJ, Conesa A, Westerhuis JA, Hoefsloot HCJ, Smilde AK, Talón M, Ferrer A. 2007. Discovering gene expression patterns in time course microarray experiments by ANOVA–SCA. Bioinformatics. 23(14):1792–1800. doi:10.1093/bioinformatics/btm251.

Park DI, Dournes C, Sillaber I, Ising M, Asara JM, Webhofer C, Filiou MD, Müller MB, Turck CW. 2017. Delineation of molecular pathway activities of the chronic antidepressant treatment response suggests important roles for glutamatergic and ubiquitin–proteasome systems. Transl Psychiatry. 7(4):e1078. doi:10.1038/tp.2017.39.

Rebai R, Jasmin L, Boudah A. 2017. The antidepressant effect of melatonin and fluoxetine in diabetic rats is associated with a reduction of the oxidative stress in the prefrontal and hippocampal cortices. Brain Res Bull. 134:142–150. doi:10.1016/j.brainresbull.2017.07.013.

Ribbenstedt A, Ziarrusta H, Benskin JP. 2018. Development, characterization and comparisons of targeted and non-targeted metabolomics methods. PLOS ONE. 13(11):e0207082. doi:10.1371/journal.pone.0207082.

Saito K, Maekawa K, Ishikawa M, Senoo Y, Urata M, Murayama M, Nakatsu N, Yamada H, Saito Y. 2014. Glucosylceramide and Lysophosphatidylcholines as Potential Blood Biomarkers for Drug-Induced Hepatic Phospholipidosis. Toxicol Sci. 141(2):377–386. doi:10.1093/toxsci/kfu132.

Schymanski EL, Jeon J, Gulde R, Fenner K, Ruff M, Singer HP, Hollender J. 2014. Identifying Small Molecules via High Resolution Mass Spectrometry: Communicating Confidence. Environ Sci Technol. 48(4):2097–2098. doi:10.1021/es5002105.

Shi B, Tian J, Xiang H, Guo X, Zhang L, Du G, Qin X. 2013. A 1H-NMR plasma metabonomic study of acute and chronic stress models of depression in rats. Behav Brain Res. 241:86–91. doi:10.1016/j.bbr.2012.11.036.

640Simmons DBD, Benskin JP, Cosgrove JR, Duncker BP, Ekman DR, Martyniuk CJ,
641Sherry JP. 2015. Omics for aquatic ecotoxicology: Control of extraneous variability to
642enhance the analysis of environmental effects. Environ Toxicol Chem. 34(8):1693–
6431704. doi:10.1002/etc.3002.

644Simmons DBD, McCallum ES, Balshine S, Chandramouli B, Cosgrove J, Sherry JP.
6452017. Reduced anxiety is associated with the accumulation of six serotonin reuptake
646inhibitors in wastewater treatment effluent exposed goldfish Carassius auratus. Sci Rep.
6477. doi:10.1038/s41598-017-15989-z. [accessed 2018 Oct 4].
648https://www.ncbi.nlm.nih.gov/pmc/articles/PMC5717243/.

649Stahl SM. 1998. Not So Selective Serotonin Reuptake Inhibitors. J Clin Psychiatry.
65059(7):333–343.

651Styrishave B, Halling-Sørensen B, Ingerslev F. 2011. Environmental risk assessment of
652three selective serotonin reuptake inhibitors in the aquatic environment: A case study
653including a cocktail scenario. Environ Toxicol Chem. 30(1):254–261.
654doi:10.1002/etc.372.

655Togola A, Budzinski H. 2008. Multi-residue analysis of pharmaceutical compounds in
656aqueous samples. J Chromatogr A. 1177(1):150–158.
657doi:10.1016/j.chroma.2007.10.105.

658Viant MR. 2008. Recent developments in environmental metabolomics. Mol Biosyst.
6594(10):980–986. doi:10.1039/B805354E.

660Vinaixa M, Samino S, Saez I, Duran J, Guinovart JJ, Yanes O. 2012. A Guideline to
661Univariate Statistical Analysis for LC/MS-Based Untargeted Metabolomics-Derived
662Data. Metabolites. 2(4):775–795. doi:10.3390/metabo2040775.

663Vismari L, Alves GJ, Muscará MN, Palermo-Neto J. 2012. A possible role to nitric
664oxide in the anti-inflammatory effects of amitriptyline. Immunopharmacol
665Immunotoxicol. 34(4):578–585. doi:10.3109/08923973.2011.638305.

666Webhofer C, Gormanns P, Tolstikov V, Zieglgänsberger W, Sillaber I, Holsboer F, Turck
667CW. 2011. Metabolite profiling of antidepressant drug action reveals novel drug targets
668beyond monoamine elevation. Transl Psychiatry. 1(12):e58. doi:10.1038/tp.2011.56.

Winder VL, Sapozhnikova Y, Pennington PL, Wirth EF. 2009. Effects of fluoxetine exposure on serotonin-related activity in the sheepshead minnow (Cyprinodon variegatus) using LC/MS/MS detection and quantitation. Comp Biochem Physiol Part C Toxicol Pharmacol. 149(4):559–565. doi:10.1016/j.cbpc.2008.12.008.

Wishart DS, Tzur D, Knox C, Eisner R, Guo AC, Young N, Cheng D, Jewell K, Arndt D, Sawhney S, et al. 2007. HMDB: the Human Metabolome Database. Nucleic Acids Res. 35(Database issue):D521–D526. doi:10.1093/nar/gkl923.

Worley B, Powers R. 2013. Multivariate Analysis in Metabolomics. Curr Metabolomics. 1(1):92–107. doi:10.2174/2213235X11301010092.

Xia J, Sinelnikov IV, Han B, Wishart DS. 2015. MetaboAnalyst 3.0—making metabolomics more meaningful. Nucleic Acids Res. 43(Web Server issue):W251–W257. doi:10.1093/nar/gkv380.

Xia Z, Ying G, Hansson AL, Karlsson H, Xie Y, Bergstrand A, DePierre JW, Nässberger L. 2000. Antidepressant-induced lipidosis with special reference to tricyclic compounds. Prog Neurobiol. 60(6):501–512. doi:10.1016/S0301-0082(99)00036-2.

Yang M, Qiu W, Chen J, Zhan J, Pan C, Lei X, Wu M. 2014. Growth inhibition and coordinated physiological regulation of zebrafish (Danio rerio) embryos upon sublethal exposure to antidepressant amitriptyline. Aquat Toxicol. 151:68–76. doi:10.1016/j.aquatox.2013.12.029.

Yaron I, Shirazi I, Judovich R, Levartovsky D, Caspi D, Yaron M. 1999. Fluoxetine and amitriptyline inhibit nitric oxide, prostaglandin E2, and hyaluronic acid production in human synovial cells and synovial tissue cultures. Arthritis Rheum. 42(12):2561–2568. doi:10.1002/1529-0131(199912)42:12<2561::AID-ANR8>3.0.CO;2-U.

Zhao Y-Y, Wang H-L, Cheng X-L, Wei F, Bai X, Lin R-C, Vaziri ND. 2015. Metabolomics analysis reveals the association between lipid abnormalities and oxidative stress, inflammation, fibrosis, and Nrf2 dysfunction in aristolochic acid-induced nephropathy. Sci Rep. 5. doi:10.1038/srep12936. [accessed 2018 Jan 11]. https://www.ncbi.nlm.nih.gov/pmc/articles/PMC4528220/.

Ziarrusta H, Mijangos L, Izagirre U, Plassmann MM, Benskin JP, Anakabe E, Olivares M, Zuloaga O. 2017. Bioconcentration and Biotransformation of Amitriptyline in Gilt-Head Bream. Environ Sci Technol. 51(4):2464–2471. doi:10.1021/acs.est.6b05831.

Ziarrusta H, Mijangos L, Prieto A, Etxebarria N, Zuloaga O, Olivares M. 2016. Determination of tricyclic antidepressants in biota tissue and environmental waters by liquid chromatography-tandem mass spectrometry. Anal Bioanal Chem. 408(4):1205–1216. doi:10.1007/s00216-015-9224-y.

FIGURE CAPTIONS

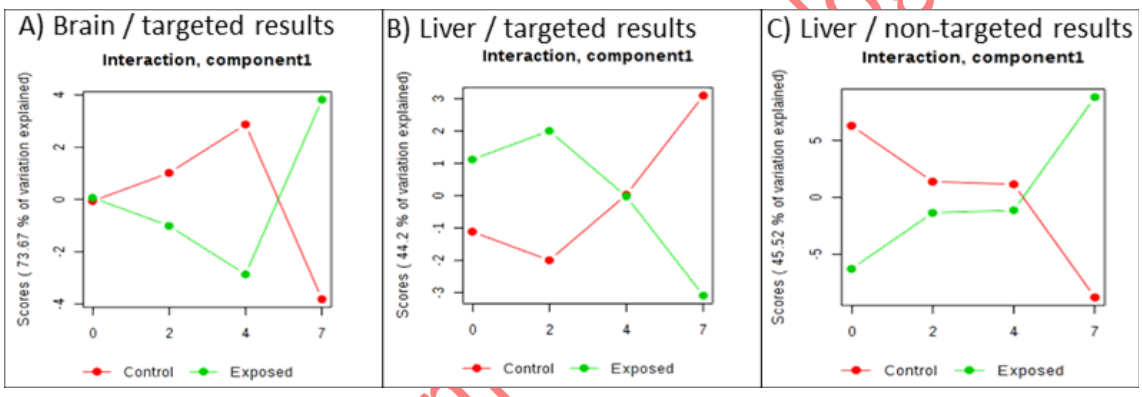

Figure 1: Score diagrams of Principal Component 1 in submodel dose·time for targeted results in brain (A), targeted results in liver (B) and non-targeted results in liver (c). Lines join the averages for each group and time point.

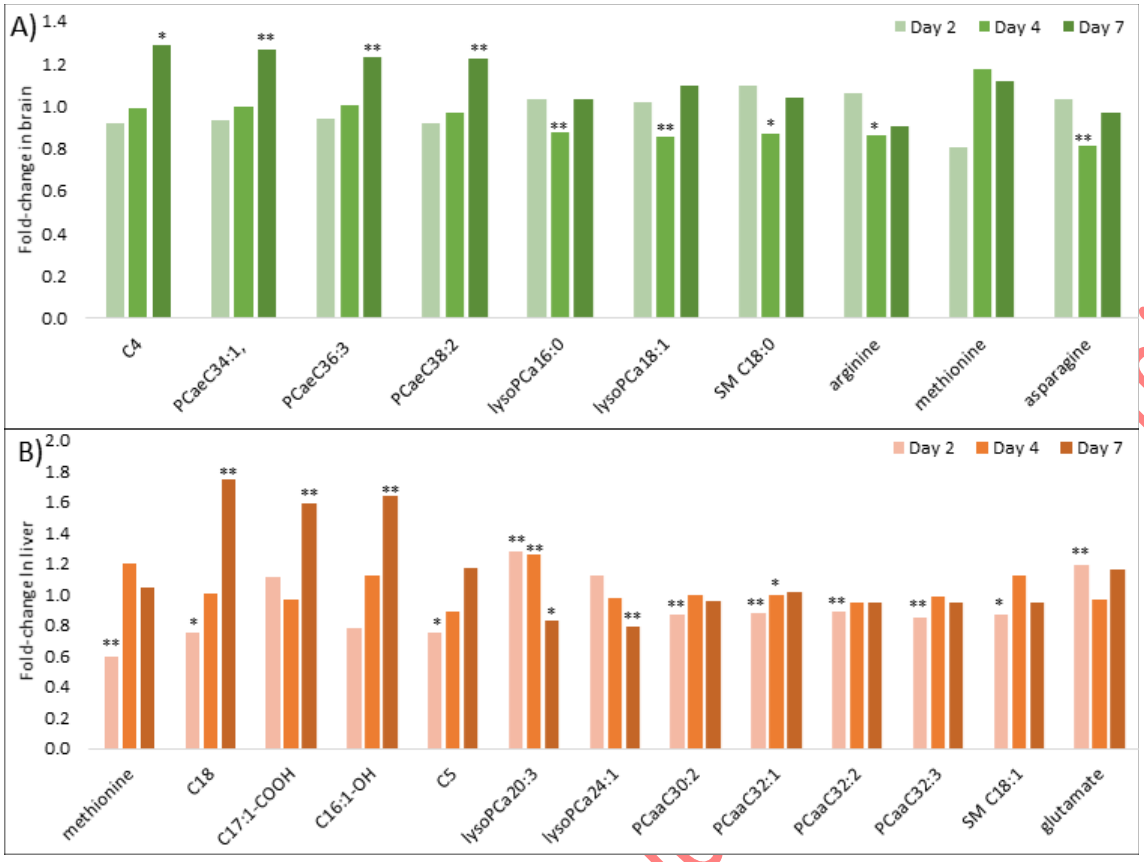

Figure 2: Fold change (FC) values of the significantly altered target metabolites after exposure according to ASCA at 2nd day, 4th day and 7th day exposure time for targeted results in brain (A) and liver (B). The fold-change (FC) values were calculated by dividing the average concentration of the metabolite in the exposed samples with the average concentration of the metabolite in the control samples at the corresponding day. Identification of the selected metabolites is given in the x-axis of the plots. *: *p-value* < 0.1; **: *p-value* < 0.05.

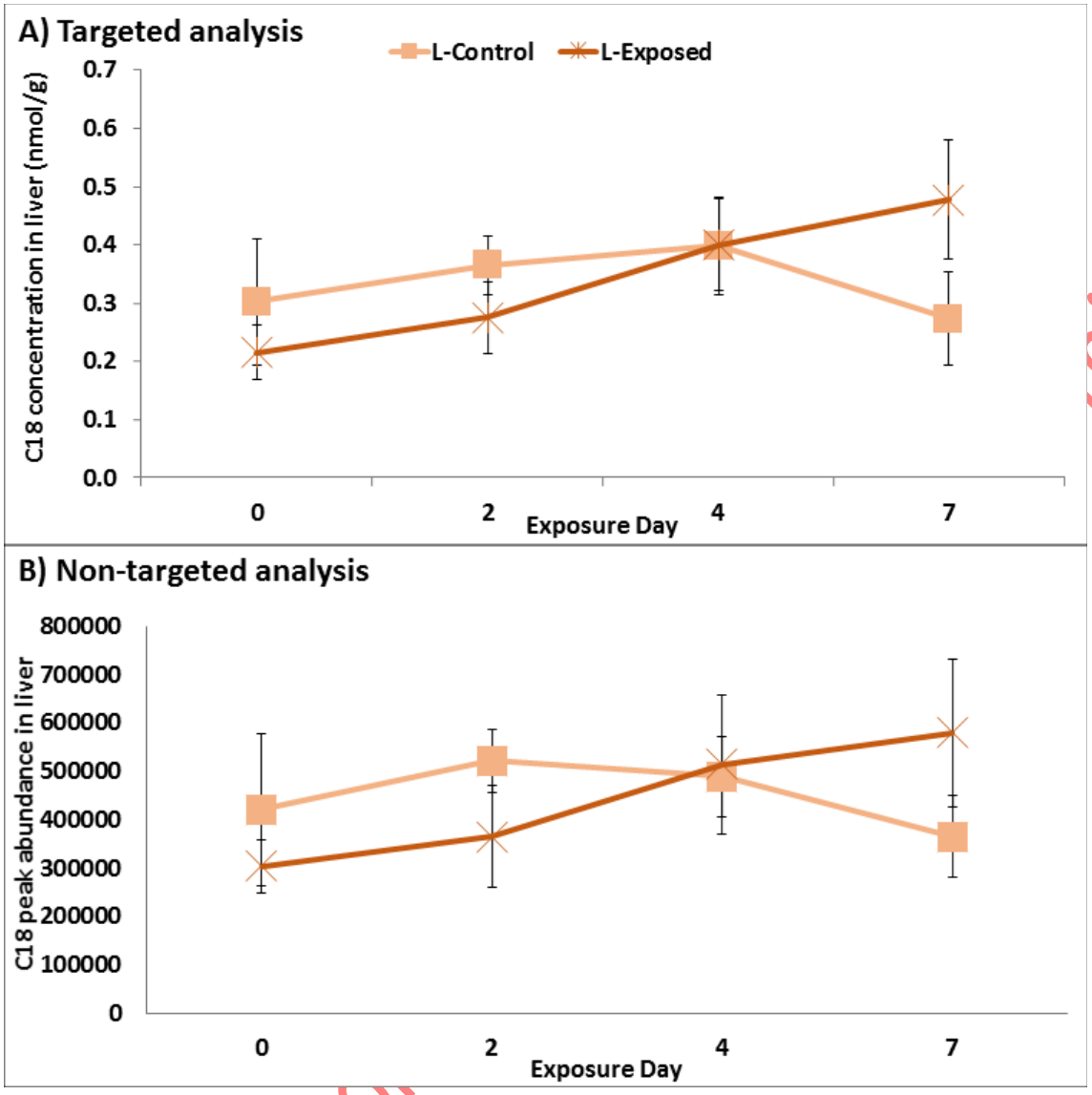

719**Figure 3:** Individual average liver concentrations (A, targeted analysis) or peak areas
720(B, non-targeted analysis) for a 95% confidence interval of C18 acyl carnitine in control
721and exposed fish through the experiment (days 0, 2, 4 and 7).

722

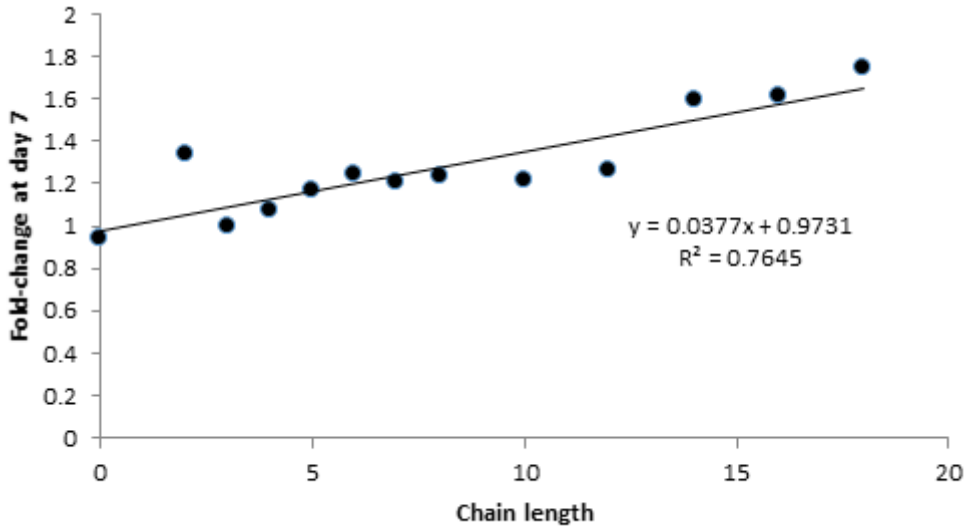

Figure 4: Correlation between chain length of saturated carnitines and the exposed/control ratio at the 7th day of exposure in fish liver. The fold-change (FC) values were calculated by dividing the average concentration of the metabolite in the exposed samples at day 7 with the average concentration of the metabolite in the control samples at day 7.

Table 1: ASCA results. Significance and explained variance for the first two principal components for the submodels dose, time and dose·time interaction of targeted and non-targeted results of the different analyzed tissues.

Tissue	Factor	Targeted results			Non-targeted results		
		Significance (p-value)	Scores explained variance (%)		Significance (p-value)	Scores explained variance (%)	
			PC1	PC2		PC1	PC2
Brain	dose	0.95	-	-	0.70	-	-
	time	0.001	60.9	28.3	<0.001	50.1	30.7
	dose·time	0.003	73.7	15.8	0.11	-	-
	Residuals		28.2	13.1		19.1	7.9
Liver	dose	0.53	-	-	0.48	-	-
	time	<0.001	73.9	19.1	0.002	53.8	27.2
	dose·time	0.03	44.2	37.9	0.03	44.5	34.2
	Residuals		20.4	14.8		12.3	7.5

Table 2: Identification of the features whose liver concentrations were significantly altered after exposure according to ASCA, their fold-change (FC) values of days 2, 4 and 7.

Peak	Molecular Weight	Name or Molecular formula	Level	Code (KEGG or LipidMaps)	Fold-Change (E/C)		
					Day 2	Day 4	Day 7
KEGG identified							
HILICpos_Peak286	219.1106	Pantothenate	2a	C00864	1.78*	0.87	1.74**
HILICneg_Peak194	168.02765	Urate	2a	C00366	1.95**	0.86	1.20
HILICpos_Peak1	174.06401	Formylisoglutamine / N-Formimino-L-glutamate	3	C16674 / C00439	5.18	0.68	3.25**
Lipid of fatty acyls category (LMFA)							
C18pos_Peak153	427.36586	C18:0 (Stearoylcarnitine)	2b	7070008	0.70**	1.05	1.59*
Lipids of sphingolipids category (LMSP)							
C18pos_Peak141	309.26659	(9Me,4E,8E,10E-d19:3) sphingosine	2b	1080014	0.94	1.05	0.66**
C18pos_Peak31	647.62106	Cer(d18:1\ /24:1(15Z))	2a	2010009	1.01	1.03	0.81**
HILICpos_Peak319	688.55202	C38H77N2O6P (2 candidates)	3	03010038, 03010037	1.11	1.05	1.44**
Lipids of sterol lipids category (LMST)							
HILICpos_Peak264	444.36093	C29H48O3 (6 candidates)	3	01010175, 01010227, 01031087, 03020419, 03020420, 03020421	0.64**	0.90	1.01
HILICpos_Peak79	368.34463	3-Deoxyvitamin D3	2b	03020618	0.73**	1.14	0.95
Lipids of glycerophospholipids category (LMGP)							
C18neg_Peak12	777.53107	C44H76NO8P (4 candidates)	3	02011139, 02011210, 01012099, 01010512	0.51**	0.90	1.09
C18neg_Peak43	453.28577	C21H44NO7P (2 candidates)	3	02050002, 01050001	0.72*	1.35	1.18
C18neg_Peak48	481.31683	C23H48NO7P (4 candidates)	3	02050001, 01050016, 01080020, 01080029	0.82**	1.12	1.20**
C18neg_Peak50	743.54682	C41H78NO8P (4 candidates)	3	02011193, 02010044, 01011618, 01010543	0.95	1.00	1.49**
C18neg_Peak52	479.30127	C23H46NO7P (2 candidates)	3	02050004, 01050125	0.78**	1.15	1.09
C18neg_Peak57	748.5257	C40H77O10P (8 candidates)	3	04010149, 04010484, 04010457, 04010178, 04010127, 04010511, 04010102, 04010530	0.61**	0.94	1.04
C18neg_Peak6	765.53077	C43H76NO8P (4 candidates)	3	02010973, 02011201, 01011425, 01011930	0.76*	0.99	1.25*
C18neg_Peak70	708.47329	C40H69O8P (2 candidates)	3	10010655, 10010240	0.75	1.34	1.74**
C18neg_Peak77	805.56258	C46H80NO8P (2 candidates)	3	01011116, 01010650	0.73**	1.02	1.10
C18pos_Peak195	453.28546	C21H44NO7P (2 candidates)	3	02050002, 01050001	0.66**	1.24	1.35**
C18pos_Peak207	479.30089	PE(18:1(9Z)\/0:0)	2b	02050004	0.81**	1.11	1.14
C18pos_Peak6	763.51454	C43H74NO8P (13 candidates)	3	02011161, 02010095, 20020014, 02011172, 02011195, 02010945, 02011192, 02010916, 02010917, 02010887, 02010759, 02010729, 02010701	0.84	1.14	1.21*
C18pos_Peak8	757.5615	C42H80NO8P (27 candidates)	3	01010592, 01010585, 01010590, 01010920, 01010588, 01010586, 01010926, 01010932, 01010589, 01011559, 01011504, 01010687, 01010678, 01010887, 01012147, 01010688, 01010727, 01010728, 01010745, 01011398, 01011449, 01011808, 01011761, 01011373, 01011837, 01012035, 01011336	1.38	1.56**	0.79
HILICneg_Peak109	835.51614	PE(22:6(4Z,7Z,10Z,13Z,16Z,19Z)\/22:6(4Z,7Z,10Z,13Z,16Z,19Z))	2b	02010093	1.14	0.95	0.77**
HILICneg_Peak38	803.56873	C43H82NO10P (15 candidates)	3	00000048, 03010332, 03010462, 03010704, 03010187, 03010157, 03010729, 03010239, 03010536, 03010318, 03010491, 03010221, 03010681, 03010266, 03010516	1.25**	1.02	0.80
HILICneg_Peak58	479.30085	C23H46NO7P (2 candidates)	3	02050004, 01050125	0.73	1.11	0.89
HILICpos_Peak16	805.56144	C46H80NO8P (22 candidates)	3	01010650, 01011116, 01012141, 01012140, 01012216, 01010844, 01012201, 01011909, 01012175, 01011880,	1.03	1.00	1.42**

Peak	Molecular Weight	Name or Molecular formula	Level	Code (KEGG or LipidMaps)	Fold-Change (E/C)		
					Day 2	Day 4	Day 7
				01012212, 01012179, 01010907, 01011851, 01012171, 01010943, 01012200, 01011721, 01011662, 01011057, 01011881, 01011691			
HILICpos_Peak17	783.57851	C44H82NO8P (19 candidates)	3	01011589, 01011651, 01011588, 01011682, 01011624, 01010895, 01012168, 01010893, 01012149, 01011766, 01011568, 01012194, 01010622, 01011872, 01010624, 01012038, 01011842, 01011490, 01011406	1.03	0.84	1.27
HILICpos_Peak187	467.30131	C22H46NO7P (3 candidates)	3	01050073, 01050012, 01020009	1.28	1.04	1.20
HILICpos_Peak193	787.51563	C45H74NO8P (7 candidates)	3	02011144, 02011191, 02011118, 02010767, 02011173, 02010926, 02010983	1.19	1.04	1.45**
HILICpos_Peak458	819.61213	C48H86NO7P (3 candidates)	3	01020110, 01090059, 01030098	1.55**	1.17	1.27*
HILICpos_Peak53	769.56366	C43H80NO8P (24 candidates)	3	01011602, 01011562, 01011423, 01011870, 02010913, 02011202, 01011533, 01011622, 01011452, 01011840, 02010647, 02010883, 01011507, 01011506, 01011679, 01011648, 02010854, 02010670, 02011078, 02010537, 02010832, 02010726, 02010831, 02010698	0.83	0.86	1.33*
HILICpos_Peak56	763.5154	C43H74NO8P (13 candidates)	3	02011161, 02010095, 20020014, 02011172, 02011195, 02010945, 02011192, 02010916, 02010917, 02010887, 02010759, 02010729, 02010701	0.95	1.24	1.89**
HILICpos_Peak57	741.53203	C41H76NO8P (24 candidates)	3	02010908, 02011222, 01011444, 01011619, 02010048, 02010663, 02010878, 02010531, 01011867, 01011355, 02010720, 02010629, 02010690, 02010628, 01011482, 01011558, 01011417, 01011416, 01011675, 01011644, 02010608, 02010803, 02011074, 02010449	0.94	1.19	1.83**
HILICpos_Peak87	803.54678	C46H78NO8P (11 candidates)	3	01010696, 01012103, 01011306, 01011634, 01011938, 01011882, 01011722, 01011910, 01011663, 01011692, 01011911	1.07	1.07	1.53**
Lipids of glycerolipids category (LMGL)							
C18pos_Peak42	402.2768	MG(0:0\/22:6 (4Z,7Z,10Z,13Z,16Z,19Z)\/0:0)	3	01010027	1.54	1.04	0.61**
C18pos_Peak54	616.50614	C39H68O5 (3 candidates)	3	02010480, 02010064,02010063	1.24	1.15	0.63**
C18pos_Peak75	638.49114	C41H66O5 (2 candidates)	3	02010174, 02010143	1.17	1.16	0.57**

*: *p-value* < 0.1; **: *p-value* < 0.05.